3D Cell Growth and Proliferation on a RGD Functionalized Nanofibrillar Hydrogel Based on a Conformationally Restricted Residue Containing Dipeptide

Jiban J. Panda,[†] Raina Dua,[†] Aseem Mishra,[†] Bhabatosh Mittra,[‡] and Virander S. Chauhan*[,†]

International Centre for Genetic Engineering and Biotechnology, New Delhi, India, and P.G. Department of Biosciences and Biotechnology, Fakir Mohan University, Balasore, Orissa, India

ABSTRACT Three-dimensional (3D) hydrogels incorporating a compendium of bioactive molecules can allow efficient proliferation and differentiation of cells and can thus act as successful tissue engineering scaffolds. Self-assembled peptide-based hydrogels can be worthy candidates for such applications as peptides are biocompatible, biodegradable and can be easily functionalized with desired moieties. Here, we report 3D growth and proliferation of mammalian cells (HeLa and L929) on a dipeptide hydrogel chemically functionalized with a pentapeptide containing Arg-Gly-Asp (RGD) motif. The method of functionalization is simple, direct and can be adapted to other functional moieties as well. The functionalized gel was noncytotoxic, exhibited enhanced cell growth promoting properties, and promoted 3D growth and proliferation of cells for almost 2 weeks, with simultaneous preservation of their metabolic activities. The presence of effective cell growth supporting properties in a simple and easy to functionalize dipeptide hydrogel is unique and makes it a promising candidate for tissue engineering and cell biological applications.

KEYWORDS: hydrogel • tissue engineering • fibers • self-assembly • dehydrophenylalanine

1. INTRODUCTION

The concept of tissue engineering allows in vitro expansion of isolated cells using cell culture techniques and their transplantation for organ regeneration. For successful tissue regeneration, it is indispensable to provide cells an environment suitable for regeneration, induction, and development of neo-tissue. Cells often behave differently when they are isolated from the complex architecture of their native tissues and constrained to petri dishes (1). There are several drawbacks of culturing cells in a two dimensional (2D) environment which include, lack of 3D molecular gradients vital for biological differentiation, organ development, signal transduction, neural information transmission, and countless other biological processes (2, 3). Other drawbacks of 2D culture conditions include altered metabolism and gene expression patterns in order to adapt to the changes in oxygen, nutrients and extracellular matrix interactions, altered production of own extracellular matrix (ECM) proteins and morphological changes (4, 5). Hence, it is necessary that cells should be provided with 3D matrix to maintain their phenotypic shape and establish natural behavior patterns. Scaffolds required for the 3D growth of cells to generate specific organs should ideally be biodegradable and result in nontoxic products easily eliminated by the host, should have an interconnected open porous network structure that permits seeded living cells to adhere and proliferate appropriately. The architecture of natural ECM components has inspired several researchers to use materials with similar structure, such as hydrogels, for cell-based therapeutics (6, 7) and soft tissue engineering scaffolds (8). Different tissues, chondrocytes (9−11), hepatocytes (12), bone marrow stromal cells (13), bone marrow-derived mesenchymal stem cells (14), and embryonic stem cells have been cultured either on surfaces or inside different hydrogels.

Hydrogels currently being developed for cell-based therapeutics are either formed from natural biopolymers (such as collagen, hyaluronate, fibrin, alginate, agarose, and chitosan) or synthetic polymers (such as poly(acrylic acid), poly(ethylene oxide), poly(vinyl alcohol), and polyphosphazene) (8). Natural biopolymers have biological functionality, are nontoxic and their gels provide endogenous signals at right scales to promote cellular interactions underlying tissue formation, but their sources are limited, properties are variable, and concerns about viral contamination can restrict their use in biomedical applications. The advantages of synthetic polymer-based gels include their consistent composition and predictable properties, but they usually lack functional sites for cellular interactions and have reduced biocompatibility.

Designer peptide based gelling scaffolds can act as promising candidates in tissue engineering and regenerative therapy (15). A biodegradable scaffold based on amino acids can be converted to nontoxic byproducts by enzymatic degradation. Moreover, peptides can be designed to incorporate diverse functionalities like specific ECM ligands

* Corresponding author. E-mail: virander@icgeb.res.in.
Received for review June 16, 2010 and accepted September 16, 2010
[†] International Centre for Genetic Engineering and Biotechnology.
[‡] Fakir Mohan University.
DOI: 10.1021/am1005173

(16−18), purified to homogeneity, and manufactured readily in large quantities. Many large peptide residue based hydrogels have been tested for their potential as appropriate tissue engineering candidates (10, 19, 20). However, most of these reported peptides were relatively large in size and lacked some desirable features such as ease of design and synthesis, facile tunability to environmental conditions, present in hydrogels based on short peptide based structures (21). Some of these issues have been addressed in hydrogels based on short N-terminus protected dipeptides (22−25). Ulijn and coworkers have further described that the compatibility of N-terminus protected dipeptide gels towards different cell types can be enhanced by modifying them with different chemical functionalities such as NH_2, COOH or OH, around fluorenylmethyloxycarbonyl (Fmoc)-Phe-Phe gel motif by just physical mixing of n-protected Fmoc amino acids (22).

In this work, we describe 3D growth of mammalian cells on a self-assembled and chemically functionalized hydrogel based on a dipeptide (26), phenylalanyl-dehydrophenylalanine (Phe-ΔPhe; hereafter denoted as F-ΔF). The gel (henceforth denoted as Dp-gel) was functionalized with an "RGD" containing pentapeptide by simple and easy to perform chemical process, for facilitating cell growth and proliferation. The functionalized hydrogel (hereafter denoted as Fn-gel) supported 3D cell growth for more than 2 weeks, with significant cell viability, spreading and growth. Although large-molecular-weight polypeptide-based gelators provide amenability for functionalization with desirable chemical moieties, our results suggested that the dipeptide-based hydrogel could be easily functionalized using simple chemical methods. Because of the free N-terminus of the constituent dipeptide, the gel also offers higher possibility for chemical end functionalization compared to other reported cell culture proficient modified dipeptide based hydrogels, which were functionalized mostly by physical means (22). In addition, incorporation of an unnatural amino acid ΔPhe, in the gelling motif would provide the hydrogel with enhanced stability to resist enzymatic degradation and hence longer cell culture half-life as compared to simple dipeptide based hydrogels (26). A simple dipeptide hydrogel with the flexibility of chemical end modification to achieve enhanced cell growth promoting properties, along with its higher enzymatic stability, is unique and could provide a convenient template for 3D cell growth with possible applications in tissue engineering and cell biology.

2. MATERIALS AND METHODS

2.1. Materials. The following materials were used: tetrahydrofuran (THF), *N*-methyl morpholine (NMM), dimethylformamide (DMF), piperidine, *N*,*N*′-Diisopropylcarbodiimide (DIPCDI), isobutyl chloroformate (IBCF), triisopropylsilane (TIPS), trifluoroacetic acid (TFA), 1,1,1,3,3,3-hexa-fluoro-isopropanol HFIP, phenol (Sigma), DL-threo-*β*-phenylserine (Sigma-Aldrich), Boc-Phe-OH, Wang's resin, Fmoc-Arg(Pmc)-OH, Fmoc-Gly-OH, and Fmoc-Asp(otBu)-OH, HOBt (Novabiochem), sodium acetate, ethyl acetate, acetonitrile (Spectrochem), anhydrous sodium sulfate, citric acid (Merck), RPMI-1640 (Invitrogen), 3-(4,5-dimethylthiazolyl-2)-2,5-diphenyltetrazolium bromide (MTT) (Sigma), bromophenol blue (Bio-Rad), *N*-(3-dimethylamionipropyl)-*N*′-ethylcarbodiimide hydrochloride (EDC), *N*-hydroxysuccinimide (NHS) (Pierce), 2-mercaptoethanol, 4-morphilinoethanesulfonic acid (MES), TOX7 assay kit (Sigma), ABSOLUTE-S SBIP Cell Proliferation Assay Kit (Invitrogen), Live/Dead Assay for cell viability kit (Invitrogen), HeL,a and L929 cells (ATCC).

2.2. Synthesis of F-ΔF. The peptide was synthesized using solution phase peptide synthesis method described earlier (26). Details of synthesis are provided in the Supporting Information.

2.3. Synthesis of RGDGG and RGEGG. The synthesis of peptides was carried out by solid phase synthesis methods using Fmoc-based chemistry in manual mode. Details of synthesis are provided in the Supporting Information.

2.4. Preparation of Dp-gel. Aliquots of 50 μL of solution of F-ΔF in HFIP (50 mg/mL) were added to different volumes of sodium acetate buffer (0.8 M, pH 7) to get final peptide concentrations between 0.2 and 1 % w/v. Mixtures were heated in boiling water bath for 15 min and cooled to room temperature to get hydrogels.

2.5. Tube Inversion Test of Gels. A hydrogel having rigid conformation should be stable enough to undergo an inversion test without any conformational change. Thus, tube inversion test was carried out to determine macroscopic gel stability. Inversion test was performed on 1 mL gel samples prepared in glass tubes at room temperature. After 30 min of gel formation, samples were inverted and monitored for deformation. A sample undergoing incomplete gel transition shows deformation in the form of flow toward the lid (lowest point of the inverted tube). A complete and stable hydrogel transition is characterized by an inversion test resulting in zero visible deformation.

2.6. Conjugation of RGDGG to Dp-gel. Pentapeptides RGDGG and RGEGG containing the cell adhesion motif "RGD" and the inactive control "RGE" were coupled to Dp-gel using aqueous carbodimide chemistry, widely used for derivatizing scaffolds with different cell adhesion motifs (27−30). In brief, EDC (0.4 mg, 2 mM) and NHS (0.6 mg, 5 mM) were added to 1 mL each of RGDGG and RGEGG solutions (1 mg/mL) in MES buffer (0.1M MES, 0.3M NaCl, pH 6.4) and incubated for 15 min at room temperature to form stable intermediates. 2-Mercaptoethanol (1.4 μL, final concentration of 20 mM) was added to quench excess EDC. The reaction mixtures were separately added to 0.1 cm thick Dp-gels at 1:1 molar ratio and allowed to react for 2 h at room temperature. After 2 h, excess reagents were removed from the gel surface with 3 rounds of PBS wash, 30 min each. Functionalized gels were aspirated, dissolved in 20 % acetic acid, lyophilized, purified on a preparative reverse phase C_{18} column using acetonitrile−water linear gradient, and analyzed by mass spectroscopy. For RGDGG derivatized gel (Fn-gel): observed mass, 753 Da; expected mass, 753.4 Da. For RGEGG derivatized gel (Re-gel): observed mass, 766 Da; expected mass, 766.97 Da.

2.7. Estimating the Percentage Conjugation of RGDGG and RGEGG with Dp-gel. Pentapeptides (1 mg/mL) were labeled with NHS modified Alexa-488 by incubating 2 mL of the peptides (1 mg/mL in MES buffer) with 10 μL of the dye (20 mg/mL in DMSO) at a 10:1 molar ratio for 2 h. The labeled peptides were separated from free dye by HPLC and conjugated with Dp-gel using standard EDC-NHS protocol mentioned above. Pentapeptide conjugated gels were then aspirated lightly and separated from free peptides by centrifuging them at 13000 rpm for 30 min. The percentage conjugation was calculated by measuring the amount of fluorescence of free peptides in the supernatants at λ_{em}= 520 nm.

Percentage conjugation = [(total fluorescence of the gel and pentapeptide before centrifugation - fluorescence of the supernatant)/total fluorescence of the gel and pentapeptide before centrifugation] × 100.

The maximal conjugation efficiency of RGDGG and RGEGG to the dipeptide-gel was found to be approximately 55% (w/w) and 51% (w/w), respectively.

2.8. Transmission Electron Microscopy. Transmission electron microscopy (TEM) of gels was carried out using uranyl acetate negative staining method. Briefly, a drop of 1 mL of Dp-gel (0.2 % w/v in 0.8 M sodium acetate buffer), was adsorbed on a 400 mesh copper grid with carbon coated formvar support, and stained with 1% uranyl acetate. Excess fluid was removed from the grid surface with a filter paper (Whatman No. 1) and the grid was air-dried at room temperature before being loaded in the microscope. TEM pictures of nanoparticles were taken in a transmission electron microscope (Tecnai 12 BioTWIN, FEI Netherlands) operating at 120 kV. Photomicrographs were digitally recorded using a Megaview III (SIS, Germany) digital camera. Image analysis to measure particle dimensions was carried out using Analysis IV (Megaview, SIS, Germany) software package. The same procedure was followed for imaging the modified gel.

2.9. Atomic Force Microscopy. Atomic force microscopy (AFM) of fδf gel was done using veeco's multimode system equipped with nanoscope 3D controller, operating in a tapping mode. The peptide gel was prepared as mentioned above. Five to ten microliters of the gel was deposited onto a freshly cleaved mica surface. The mica surface with the adsorbed peptide was then dried at 95% relative humidity (in a humified chamber) and observed under the microscope immediately. AFM scans were taken at 512 × 512 pixel resolution and produced topographic images of the samples, in which the brightness of features increases as a function of height.

2.10. Inflow of Bromophenol Blue into the Dipeptide Gel. Two milliliters of Dp-gel (0.5% w/v in 0.8 M sodium acetate buffer) was prepared in a test tube and covered with 10 mL of phosphate buffered saline (PBS) containing 0.1 mg of bromophenol blue. Dye inflow into the gel was monitored after regular intervals, by taking out 1 mL of the overlying solution and measuring intensity of absorption peak of the dye at 595 nm. The diffusion coefficient (D) of the dye in the gel was calculated as described earlier (26) using the nonsteady state diffusion model equation given below:

$$M_t/M_\infty = 4(Dt/\pi\lambda^2)^{1/2}$$

Where M_t is the total amount of molecules absorbed during the measurement, M_∞ is the total amount of molecules added to the overlying solution, λ represents the hydrogel thickness, t is the time of measurement, and D is the diffusion coefficient of the molecule. The same procedure was used to determine D in Fn-gel.

2.11. Stability of Dipeptide Gel. One milliliter hydrogel samples were prepared in glass tubes and incubated with 5 mLl of cell culture supernatant at 37 °C for a period of 14 days. The culture supernatant was changed every 48 h to maintain fresh stock of proteases. Tube inversion tests were carried out after fixed intervals to determine macroscopic gel stability. TEM imaging of treated (incubated with cell culture supernatant for 14 days) and untreated gels stained with uranyl acetate was used to visualize any morphological change occurring in the gel matrix at microscopic level.

2.12. Cell Viability Assay. HeLa (ovarian cancer) and L929 (mouse fibroblast) cells were obtained from ATCC and maintained in RPMI 1640 supplemented with 10% fetal calf serum, 100 units/ml penicillin and 100 μg/mL streptomycin. Cells were maintained on tissue culture treated polystyrene (TCTP) plates at 37 °C in a humified atmosphere containing 5% CO_2. Subconfluent cells were trypsinized, harvested, and counted using a hemocytometer. The resulting cell suspension was diluted in RPMI 1640 (supplemented with 10% fetal calf serum) before addition to the hydrogels. 50 μL of dipeptide gels (0.5% w/v in 0.8 M sodium acetate buffer at pH 7) were prepared in 96-well plates, washed thrice with 200 μL of PBS, 30 min each, and preconditioned with 200 μL of complete RPMI media overnight. Next day, media was removed and cells (5×10^4) from each group were seeded evenly over hydrogels. Cells were plated in triplicates on Fn-gel, Dp-gel, and Re-gel and on control TCTP plates. Culture medium was changed every other day. Viability of cells on gels was determined using the traditional MTT assay, after culture durations of 1 and 14 days. Cell morphology on gels was examined by light microscopy at 24, 72, and 14 days after seeding.

2.13. Live/Dead Cell Viability Assay. Cells were plated in triplicate (1×10^5 cell/well in 6 well plates) on control TCTP culture plate, Dp-gel and Fn-gel. Plates were incubated in 5% CO_2 at 37°C for 1 and 14 days to allow cell attachment and spreading to occur and live/dead cell viability assay was done using "Live/Dead Assay for cell viability kit" (Invitrogen) as per the manufacturer's instructions. Details of the assay are provided in the Supporting Information.

2.14. Confocal Microscopy. Cells (5×10^4 cells/well in 8-well slides) were cultured on TCTP plates, Dp-gel, and Fn-gel for desired periods. Before analysis, cells were stained with calcein AM for facilitating detection of viable cells inside the gel matrix. Confocal microscopy was carried out on a Nikon TE 2000E microscope equipped with 40×/0.6 NA Plan Fluor DIC objective lens. Calcein was excited at 488 nm with an argon ion laser and emission was recorded through emission filter set 515/30. Equidistant Z-stack images (1 μm apart) were collected in different focal planes, spanning the entire scaffold depth (1000 μm). Images were acquired, with a scanning mode format of 512 × 512 pixels. Each image was a 3D reconstruction of a series of Z-stack images (both for fluorescence and differential interference contrast (DIC) microscopy) using Image-Pro Plus version 6.0, a commercially available software package from Media Cybernetics. The number of viable cells growing in a 3D manner inside Fn and Dp gels and on TCTP plates were quantified using Image J software.

2.15. Alkaline Phosphatase (ALP) Activity Assay. The ALP activities of cells grown on the hydrogels were determined using ALP activity staining kit (Sigma), 7 days after cell seeding and growth. In cells with positive ALP activity, naphthol AS-MX was liberated and got immediately coupled with diazonium salt, forming an insoluble visible pigment at sites of phosphatase activity. Diazonium salt and naphthol AS-MX phosphate (3-hydroxy-2-naphthoic acid 2, 4-dimethylanilide phosphate) alkaline solutions were prepared as described in the manufacturer's protocol. Cells were plated in triplicate (1×10^5 cells/well in 6-well plates) on TCTP culture plate, Dp-gel, and Fn-gel. Plates were incubated in 5% CO_2 at 37 °C for 7 days to allow cell attachment and spreading to occur. Cells were then fixed in the provided fixative and incubated in the alkaline dye mixture for 30 min at 18−26 °C in dark. After this, the dye was removed, cells were rinsed with deionized water, and counter stained with Mayer's hematoxylin solution for 10 min before being observed under microscope for ALP activity.

2.16. LDH Assay. This assay is based on the reduction of NAD (Nicotinamide adenine dinucleotide) by the action of LDH (lactate dehydrogenase). The resulting reduced NAD (NADH) is utilized in the stoichiometric conversion of a tetrazolium dye into a colored compound that, measured spectrophotometrically, indicates the degree of inhibition of cell growth (cytotoxicity) caused by the test material. Cells were plated in triplicate (5×10^4 cells/well in 96-well plates) on TCTP culture plate, Dp-gel, and Fn-gel. Plates were incubated in 5% CO_2 at 37°C for 7 days to allow cell attachment and spreading to occur. Cultures were removed from incubator and placed in laminar flow hood or other sterile work area and 1/10 volume of LDH assay lysis solution was added per well and the plates were further

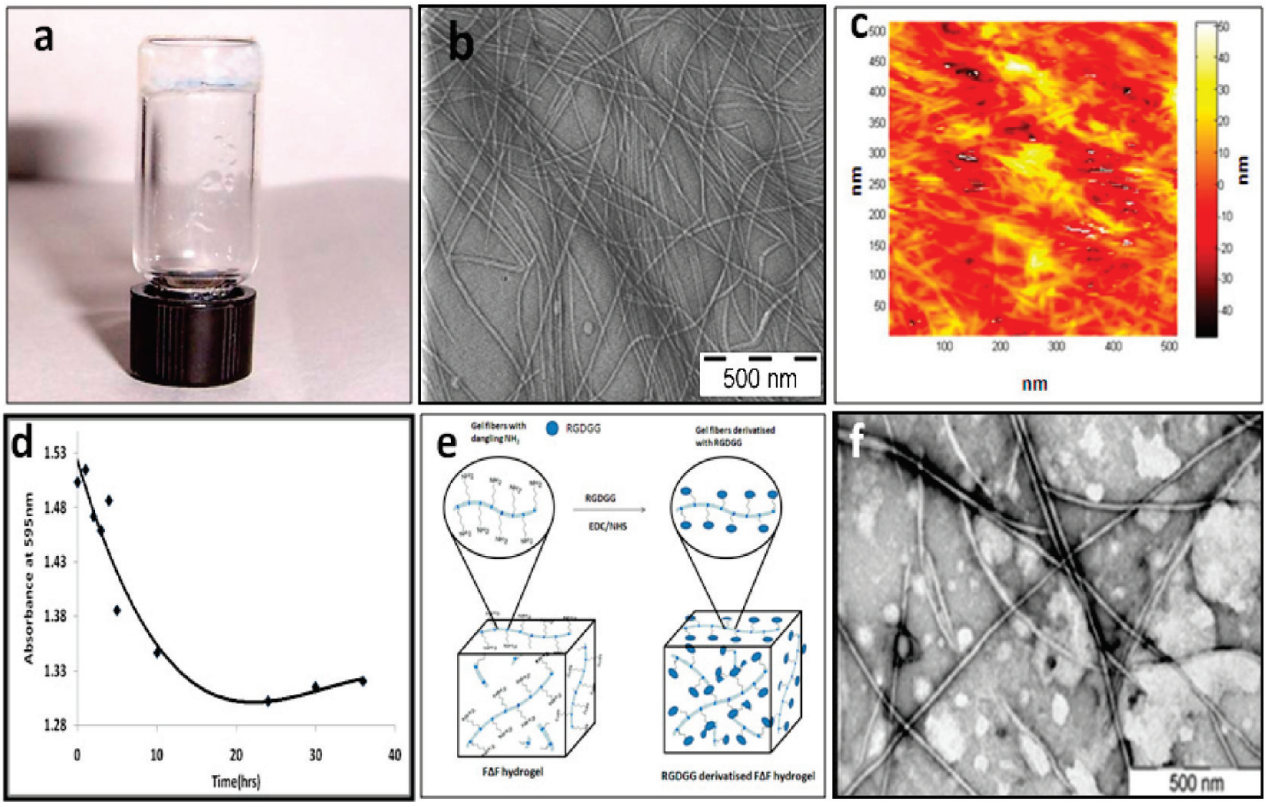

FIGURE 1. (a) Self-supporting F-ΔF gel (Dp-gel). (b) Electron microscopic image and (c) atomic force microscopic image of Dp-gel showing fibrillar network like structure of the gel matrix. (d) Inflow of bromophenol blue into the dipeptide gel (decrease in absorbance of dye in the overlying buffer indicates partitioning of the dye into the gel matrix). (e) Scheme showing conjugation of RGDGG to FΔF gel. (f) Transmission electron micrographs of FΔF gel conjugated with RGDGG (Fn-gel) showing retention of the fibrillar morphology. Scale bar: 500 nm.

incubated at 37 °C for 45 min and centrifuged at 250*g* for 4 min to pellet debris. Aliquots were transferred to clean flat-bottom plates. LDH cofactor and LDH assay mixture was prepared according to the TOX 7 protocol (Sigma Aldrich) and added in an amount equal to twice the volume of medium. The plates were covered with an opaque material to protect from light and incubated at room temperature for 20−30 min. Reaction was terminated by adding 1/10 volume of HCl (1N) to each well and absorbance was measured at a wavelength of 490 nm. Background absorbance of multiwell plates was measured at 690 nm.

Percentage LDH activity = (LDH activity of cells grown on gel/LDH activity of cells grown on TCTP control plate) × 100.

2.17. Statistical Analysis. All experiments were performed at least three times or more. Graphical results are representative data sets performed in quadruplicate. All values are expressed as means ± standard deviation.

3. RESULTS

3.1. Preparation and Characterization of F-ΔF Hydrogel. The peptide F-ΔF (see the Supporting Information, Figure 1) assembled into a 3D self-supporting hydrogel on heating and subsequently cooling a minimum of 0.2% w/v peptide suspension in 0.8 M sodium acetate buffer at pH 7 (see the Supporting Information, Figure 2). The dipeptide gel was colorless and translucent in appearance, and possessed high mechanical strength (26). A successful tube inversion test confirmed stable macroscopic hydrogel formation (Figure 1a). Tube inversion tests further showed that the gel formation was concentration dependent and highly stable gels were formed at a peptide concentration greater than 0.2% w/v (see the Supporting Information, Table 1). However, self assembled free-flowing structures with tubular morphology were formed at a peptide concentration below 0.2% w/v (31). The gel also exhibited birefringence on congo red staining, suggesting the existence of a dense network of stackable moieties (26).

3.2. Morphological Analysis of Dp-gel. TEM and AFM (Figure 1b, c) images showed that the macroscopic gel matrix was composed of a highly dense network of fibers. Each fiber was 15−20 nm in diameter with length in micrometers. The gel had highly interconnected porous networks (see the Supporting Information, Figure 3), suitable for proliferation and differentiation of cells. To assess absorbing capacity of the gel, dye intake method was used as described earlier (24). Inflow of bromophenol blue from the overlying aqueous solution to the gel was tested using UV−visible spectroscopy. The gel could absorb the dye from covering solution and turned blue. Absorbance of the dye in overlying solution showed a sharp decrease up to 10 h (due to uptake of dye by the gel) followed by a plateau thereafter (Figure 1d). The nature of the curve suggested that the rate of dye inflow was fast in earlier time points (before 10 h) and the dye could easily diffuse inside the gel with a D of 3.7×10^{-10} m^2/s.

3.3. Functionalization of Dp-gel with RGD Motif. To achieve improved cell adhesion to fibrous matrix of the gel, we covalently linked Dp-gel with a pentapeptide, RGDGG, containing the well-established cell adhesion motif,

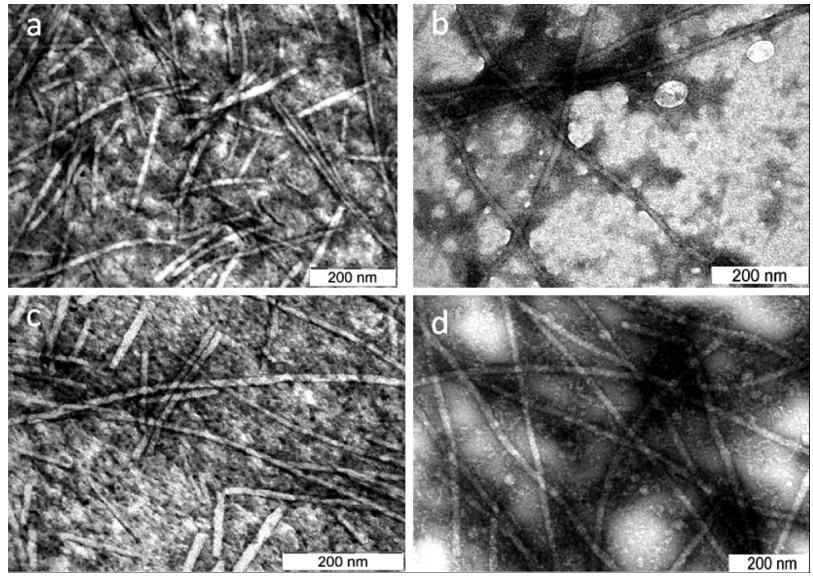

FIGURE 2. Electron micrographs showing proteolytic stability of dipeptide gels treated with cell culture supernatant. (a) Untreated Dp-gel. (b) Dp-gel treated with cell culture supernatant for 14 days. (c) Untreated Fn-gel. (d) Fn-gel treated with cell culture supernatant for 14 days. Images show stability of gel fibers to degradation by proteases present in cell culture supernatant.

RGD (32), by using aqueous carbodimide chemistry, used earlier for derivatising scaffolds with cell adhesion motifs (27−29) (Figure 1e). The pentapeptide derivatized gel (Fn-gel) was characterized by HPLC and mass spectrometry. Modified dipeptide, as expected, showed an increase in retention time on HPLC (29 min for the modified versus 26 min for the free peptide; see the Supporting Information, Figure 9a). ESI-MS analysis of the modified dipeptide showed a mass of 753 Da (see the Supporting Information, Figure 9b), which confirmed covalent linkage of the pentapeptide with the dipeptide. Moreover, electron micrographs of Fn-gel showed fibrillar architecture (Figure 1f) with an average fiber diameter of 17 nm similar to that of Dp-gel (see the Supporting Information, Table 2 and 3). To test whether the modification of Dp-gel with the pentapeptide RGDGG led to any change in diffusivity of molecules inside the functionalized gel, we determined D of bromophenol blue. D of bromophenol blue inside the functionalized gel was almost similar to that of the free gel with a value of 5×10^{-10} m^2/s. This suggested that Dp-gel was stable to functionalization with short peptides and that derivatization with RGDGG did not alter basic fibrillar morphology and related properties of the gel.

3.4. Stability of Dipeptide Gels. To determine the potential of gels as scaffolds for long term cell culture, their stability towards non-specific proteases present in the culture media was examined by incubating them with used cell culture supernatant. Both the derivatized and free dipeptide gels showed remarkable stability to degradation by proteases present in culture supernatant even after 14 days of incubation. Electron micrographs of the gel matrix before and after protease treatments showed no observable change in the tubular ultrastructure (Figure 2). Stability studies at a macroscopic level demonstrated that the overall 3D architecture of both hydrogels (Fn and Dp) were also stable (could resist tube inversion) to cell culture supernatant treatment (see the Supporting Information, Figure 10). However, after 6−7 days of incubation, small gel flakes formed because of partial disintegration of gels during this period (see the Supporting Information, Figure 11).

3.5. Cell Growth and Viability Assays on Dp and Fn Gels. Optical microscopy images of HeLa cells grown on 96 well plates coated with Dp-gel and Fn-gel for a period of 24 h, showed cells with a somewhat rounded morphology. (see the Supporting Information, Figure 12a−c). Optical micrographs, as expected, showed higher cell density in the case of Fn-gel in comparison to Dp-gel (see the Supporting Information, Figure 12b,c). However, we were unable to quantify cell numbers growing on the gels because of strong interference from the gel matrix as well as the 3D growth pattern of cells. To assess the effect of gels on the morphology of cells, we cultured cells two-dimensionally on plates coated with thin layers of gels. As gels were translucent, this facilitated proper visualization of cells under an optical microscope. Optical bright-field images so obtained showed that cells had spreaded morphology on gels as compared to the control TCTP plates (Figure 3). Cytotoxicity of gels was also qualitatively investigated using live/dead cell viability assay after 24 h of growth on the gel matrix. In this assay, calcein AM hydrolysis in live cells produced a green fluorescent signal while EthD-1 is excluded from live cells and produced a red fluorescent signal only in compromised cells. Results of this assay showed that majority of cells fluoresced green and were viable on Fn and Dp gels in a way similar to that of control TCTP plates (see the Supporting Information, Figure 13). This suggested that both gels were biocompatible and permitted cell growth.

MTT assays to quantitatively probe for viable cell densities growing on gels revealed higher cell density on Fn-gel with an optical density (OD) of 0.41, compared to an OD of 0.35 on Dp-gel (Figure 4). Similarly, L929 cells grown on gels for a period of 24 h also showed substantial growth with higher

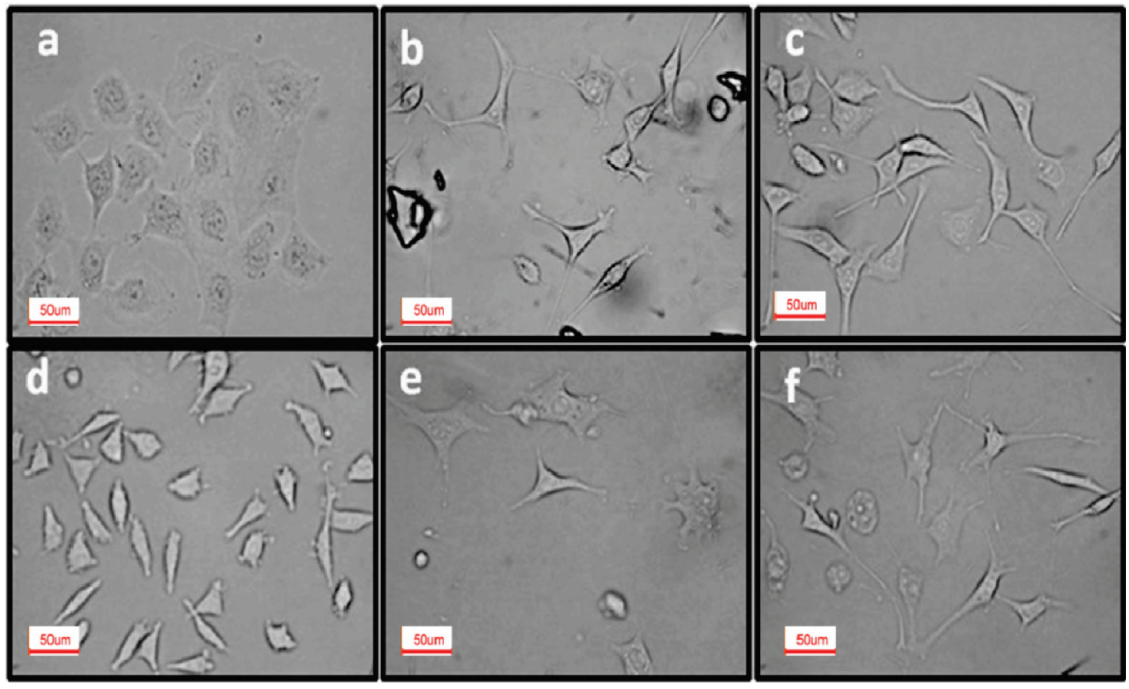

FIGURE 3. Optical images of HeLa cells cultured on (a) TCTP (b) Dp-gel (c) Fn-gel for 72 h; L929 cells cultured on (d) TCTP, (e) Dp-gel, (f) Fn-gel for 72 h. Images show spreaded and healthy morphology of the cells when cultured on the gels. Fn-gel showed higher number of attached cells than Dp-gel at a given field. Magnification: 40×.

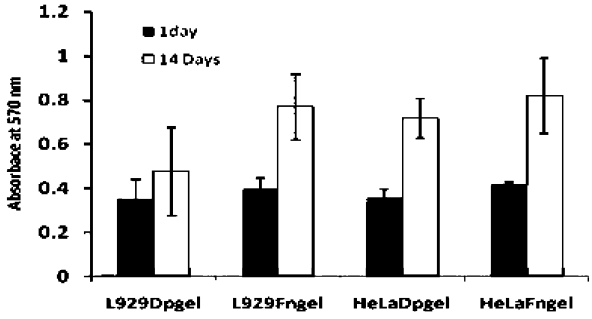

FIGURE 4. Cell viability on Dp and Fn gels. For measurement of cell viability over time, the reduction of yellow colored MTT (3-(4,5-Dimethylthiazol-2-yl)-2,5-diphenyltetrazolium bromide into purple formazan by mitochondrial reductase was monitored spectrophotometrically at 570 nm. The measured absorbance of each sample represents cellular metabolic reduction and hence cell's relative survivability. Error bars represent standard deviation; $n = 3$ for each data point. Graph show higher cell viability on Fn-gel than Dp-gel after 14 days of culture.

cell viability on Fn-gel (see the Supporting Information, Figure 12d,e, and Figure 4). To show specificity of RGDGG in promoting cell adhesion, we also conjugated a control pentapeptide, RGEGG, to FΔF gel and studied the growth of HeLa or L929 cells on the derivatized gel using MTT assay. Results showed that in both cell lines, Re-gel had similar cell density as that of free gel, which was significantly smaller than Fn-gel (see the Supporting Information, Figure 14).

We next tested for the cell growing potential of dipeptide gels over longer culture durations and carried out cell growth studies for a period of 14 days. Bright-field optical microscopic images of L929 and HeLa cells cultured on Fn-gel for 14 days showed higher cell density on Fn-gel than Dp-gel (see the Supporting Information, Figure 15b,c,e,f). Similarly, results of MTT assay of cells grown on Fn-gel for 14 days showed high cell density with an OD of ∼0.77 for L929 and ∼0.81 for HeLa, compared to an OD of ∼0.47 for L929 (almost half of those grown on Fn-gel) and ∼0.71 for HeLa in case of cells grown on Dp-gel (Fig 4).

Fluorescent microscopic images of live/dead cell viability assay carried out after 14 days of cell culture also demonstrated higher density of viable cells (those exhibiting green fluorescence) with healthy and spreaded morphology on Fn-gel than Dp-gel (Figure 5a−d). FACS analysis further revealed that HeLa cells exhibited higher viable cell population (4100 ± 150 cells) when cultured on Fn-gel than on Dp-gel (3400 ± 100 cells) (see the Supporting Information, Figure 16 and Table 4). Similar results were obtained with L929 cells when cultured on Dp and Fn gels (data not shown).

3.6. Three-Dimensional Growths of Cells on Fn and Dp Gels. To probe if cultured cells grew only on the surface or they invaded deep into the gel, we obtained confocal Z-stacking images of L929 and HeLa cells cultured on both Fn-gel and Dp-gel. 3D images were generated from a stack of laser confocal microscopy scans of 1 μm increments over total thickness of 1000 μm. In all cases, cells grown on TCTP plates were taken as control. Cells were stained with calcein-AM, for aiding visualization inside the gel matrix. Viable cells were observable after calcein-AM uptake and internal modification to fluorescent calcein. We found that while cells grew in one or two layers in TCTP plates (see the Supporting Information, Figure 17a,d), they invaded inside and grew in all three planes, *X*, *Y*, and *Z*, in both Fn-gel (Figure 6a,b) and Dp-gel (see the Supporting Information, Figure 17b−d,f).

Three-dimensional projections allowed viability analysis through the depth of Z-stacks and showed that there were

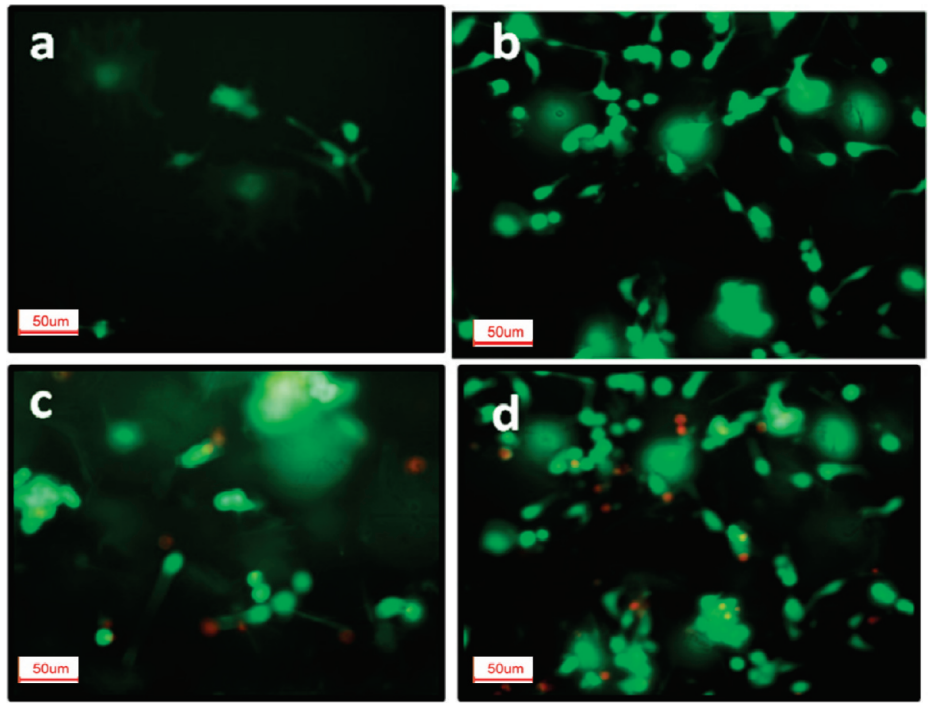

FIGURE 5. Live/dead cell viability staining images of (a) L929 cells on Dp-gel, (b) L929 cells on Fn-gel, (c) HeLa cells on Dp-gel, (d) HeLa cells on Fn-gel, after 14 days of culture. Scale bar, 50 μm; magnification, 20×. Images show healthy cells with spreaded morphology and higher cell density on Fn-gel than Dp-gel.

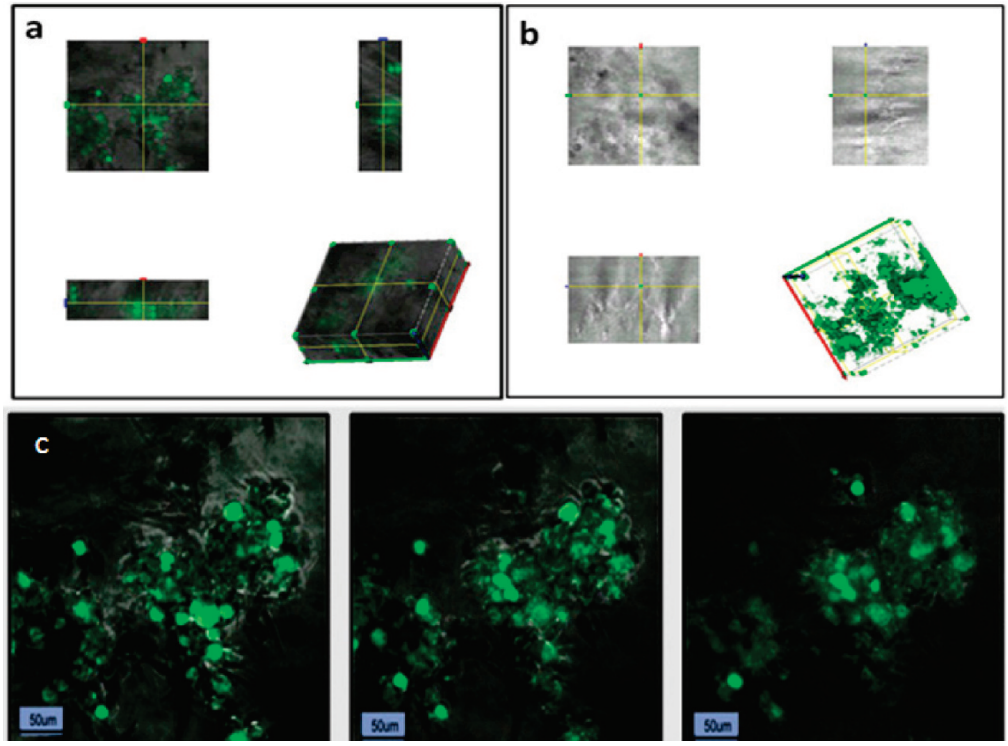

FIGURE 6. Three-dimensional volume rendering images of L929 and HeLa cell/hydrogels after 24 h of culture, generated from a stack of laser confocal microscopy scans of 1 μm increments over total thickness of 1000 μm. Cells were cultured in presence of calcein-AM prior to imaging and detected as a green emission. Images show 3D growth of (a) L929 cells and (b) HeLa cells, on Fn-gel. (c) Different confocal Z-stack images of L929/Fn-gel after 7 days of culture. (Left) Stack 63 with 55 viable cells, (middle) stack 115 with 74 viable cells, (right) stack 140 with 79 viable cells (stacks were spaced 1μm apart). Images show presence of viable cells (L929) throughout the 3D scaffold. Scale bar, 50 μm; magnification, 20×.

viable cell clusters throughout gels which stained positive for calcein-AM (Figure 6c). Length of the cell loaded *Z*-axis, an index of cell penetration and layering, was also higher in case of Fn-gel (see the Supporting Information, Figure 17c, f and Table 5) than Dp-gel (3.5 times higher in HeLa and 1.3 times higher in L929) and the control (8 times higher in HeLa and 2.3 times higher in L929; see the Supporting Information Figure 17a,b,d,e, and Table 5), suggesting better cell

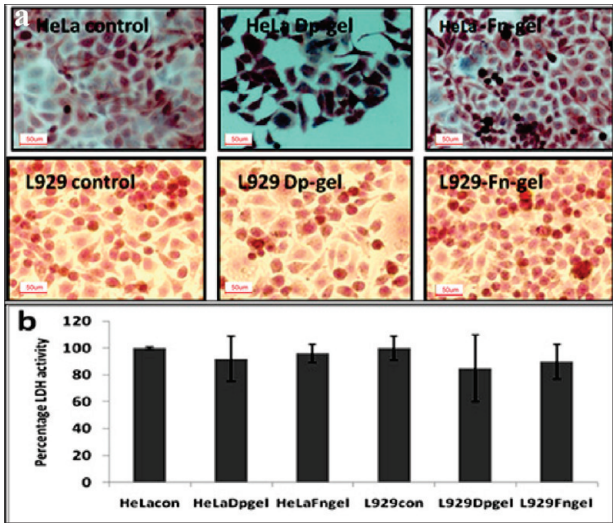

FIGURE 7. (a) Metabolic activities of mammalian cells grown on the gels monitored through ALP activity. In cells with positive ALP activity naphthol AS-MX was liberated and got immediately coupled with diazonium salt, forming an insoluble visible pigment at sites of phosphatase activity. Positive ALP activity is seen in all cases. (b) Percentage LDH activity of cells grown on TCTP culture plate, Dp-gel, Fn-gel, for 7 days. This assay is based on the reduction of NAD by the action of LDH. The resulting reduced NAD (NADH) is utilized in the stoichiometric conversion of a tetrazolium dye into a colored compound which, measured spectrophotometrically indicates the degree of inhibition of cell growth (cytotoxicity) caused by the test material. The percentage LDH activity (materials methods) indicates presence of active enzyme in all the three cases. Magnification, 20×.

invasion into the derivatized gel. Number of viable cells growing in a 3D manner inside Fn and Dp gels was also quantified using Image J software and it was observed that the number of viable L929 cells growing on Fn-gel was 1.7 fold higher than Dp-gel and 4 fold higher than control TCTP plates. Similarly, the number of HeLa cells growing on Fn-gel was 1.6 times higher than Dp-gel and 5 times higher than TCTP plates (see the Supporting Information, Table 6).

3.7. Metabolic Activity Assays. Metabolic activities of cells growing on TCTP plates and the two dipeptide gels were probed using standard enzymatic assays like ALP activity assay, LDH assay and MTT assay. Alkaline phosphatase activity assay showed positive staining in all three cases, suggesting that cells were metabolically active inside gels (Figure 7a).

Conventionally used LDH and MTT assays were carried out to provide a quantitative measure of cellular metabolism in cells cultured on TCTP plates and the two dipeptide gels (23, 33). Cells exhibited similar percentage of LDH activity in all three cases (Figure 7b) revealing the presence of the metabolically active marker enzyme. MTT assay also revealed the presence of active mitochondrial reductases which reduced yellow colored MTT to purple formazan giving absorbance at 570 nm in cells cultured on the dipeptide gels (Figure 4).

4. DISCUSSION

A dipeptide containing a conformational constraining residue ΔF was shown to form a self-assembled and self-supportive hydrogel with high mechanical strength (Dp-gel) at a peptide concentration greater than 0.25% w/v. In fact, it was somewhat surprising to observe the formation of hydrogel at a concentration ≥0.25% w/v from a simple dipeptide that self-assembled into well-defined, stable tubular structures at a concentration of 0.1% w/v (31). Exact process by which gel formation takes place is not clear to us. Whether, gelation is a two- or single-step process, i.e., if tubular structures are first formed and then converted to fibrillar structures leading to gel formation or gelation occurred directly, needs to be investigated further. The gel had nanodimensions and was noncytotoxic and stable under cell culture conditions (26). Moreover, as the dipeptide hydrogel gel demonstrated sensitivity to different factors like mechanical forces, environmental changes such as salt, pH, and temperature (26). Use of one or more of these treatments could enable disintegration of the gel and facilitate its removal from the culture system. These properties of the gel as well as the ease of preparation, prompted us to explore its potential as a scaffold for 3D growth of cells.

Morphological analysis of both Dp-gel and Fn-gel demonstrated that the gels had fibrillar structures with nanodimensions, which imparted them with high surface to volume ratio; a property crucial for a scaffold to accommodate large number of cells. Nanodimensions of the constituent fibers also provided a suitable medium for cells to interact with, for their proper growth and differentiation (34−36). Dipeptide gel matrix described here exhibited an interconnected porous network like structure that would allow free diffusion of nutrients and waste materials (37, 38), making it a suitable cell culture matrix candidate. Bromophenol blue infiltration assay also suggested that the architecture of the gel could allow absorption of nutrients from the culture media, needed to promote 3D growth of cells. Similar results were recently reported for another hydrogel also based on a phenylalanine containing dipeptide, but with a bulky aromatic N-terminal, Fmoc, protecting group (24).

Many anchorage-dependent cell types used in tissue engineering form a tight mechanical binding to scaffolds as their initial cellular level interactions (39) wherein integrin is known to promote cell adhesion and spreading for cell survival and proliferation (40, 41). By design, the constituent dipeptide (FΔF) of Dp-gel has its amino terminus free which is amenable to functionalization with a variety of ligands by simple chemical procedures. We derivatised the gel chemically in aqueous conditions with synthetic pentapeptides, RGDGG, containing the well known cell adhesion motif, RGD (32), along with a diglycine linker, as well as with a mutant pentapeptide, RGEGG. The method of functionalization was simple and direct with high conjugation efficiency and was achieved without compromising the basic fibrillar morphology of the dipeptide gel. This method can be easily adapted for conjugation of variety of ligands with the free amino group of the gel as well.

A scaffold to be used for 3D growth of cells should ideally be stable to different culture conditions, in order to allow cell growth and proliferation for a desired period. At the same time, it should be flexible enough to facilitate cell

migration and proliferation inside the scaffold. Although, both free and functionalized dipeptide gels were stable to degradation by proteases present in the cell culture supernatant, partial gel disintegration (possibly occurring due to change in media pH (26) with progressive cell growth or slow proteolytic degradation of the peptide) was visible after 6−7 days of incubation. This partial disintegration leading to loosening of the gel is likely to assist cell migration and growth inside the gel matrix.

For the proof of concept, two standard and readily available adherent cell lines, HeLa and L929, were chosen for cellular growth studies. After 24 h of growth, both HeLa and L929 cells remained viable on Fn-gel and Dp-gel with cell densities comparable to that of TCTP plates. This also implied that the gels were not cytotoxic and hence suitable for tissue engineering and other biological applications. During this period, cells exhibited rounded morphology on gels with no significant difference in viability on the derivatised or free gels. However, results of MTT reduction assay carried out after longer culture durations (14 days) showed almost two-fold higher viability of L929 cells on Fn-gel than Dp-gel. Quantitative analysis of live/dead cell viability assay carried out after 14 days also showed significantly higher density of viable cells on Fn-gel as compared with underivatised gel. It was likely that, the cells needed some time to adapt and attach to the functionalized gel, leading to the insignificant difference in their viability on both the gels after 24 h of culture. Earlier studies with cell adhesion molecule functionalized hydrogels have also shown minor differences in cell attachment and growth between the derivatised and underivatised gels at initial 24 h, but significant differences after longer periods (22, 42, 43).

Additionally, after long culture durations, cells showed better attachment with spreaded morphology on the derivatized gel, whereas only a few attached cells were found on the underivatized gel. Thus, Fn-gel exhibited enhanced growth in terms of both cell viability and physical appearance, compared to control TCTP plates and Dp-gel. Similar spreaded morphology and enhanced growth has been demonstrated earlier in cell culture studies carried on designed peptide based scaffolds (44, 45), or other polymeric matrices derivatized with cell adhesion ligands (39, 46). Taken together, these results indicated that functionalization of the dipeptide gel with the cell adhesion motif, RGD, makes it a suitable scaffold for cell growth. Also, growth-promoting properties were specific to RGDGG and were not found in case of Dp-gel functionalized with other mutant pentapeptide, RGEGG, where the cell adhesion motif, RGD, was compromised by replacing the amino acid D with E.

We further found that cells (HeLa and L929) grew on both Fn-gel and Dp-gel by invading and migrating into all three (*X*, *Y*, *Z*) planes resulting in a 3D growth. Also, Fn-gel had longer cell loaded *Z*-axis, suggesting better cell penetration and growth than Dp-gel and the control. Additionally, Fn-gel had a higher number of three-dimensionally growing cells as compared to Dp-gel and TCTP plates highlighting its appropriateness as a 3D growing scaffold. Such cell migration and 3D growth which has been demonstrated in other artificial hydrogels developed for cell culture (24, 47), is a significant property and is decisive in determining the structure and growth rate of bioartificial tissues (48) developed from cell-based scaffolds and would advance cell biological studies. Results of MTT, LDH, and ALP assays, designed to test metabolic activities of cells inside different constructs (49−51), confirmed that the dipeptide gels not only favored cell proliferation and growth for a considerable time period, but also preserved their basic cellular metabolic activities**.** It is important to note that though the two cell lines showed positive cell viability, metabolic activity and healthy growth patterns on Fn-gel, no significant difference was observed between their growth rates on the hydrogel. This may be attributed to the immortal nature common to both of them.

Though short peptides containing aromatic residues that readily form gels have been recently described as scaffolds for cell growth (22−25), these peptides had their N-terminus blocked with large protecting groups, thereby making them unsuitable for chemical functionalization at the amino terminus. Although, attempts have been made to functionalize such gels with different chemical functionalities, such as NH_2, COOH, or OH by physical mixing of basic or acidic amino acids (22). Yet, the dipeptide described here has its N-terminus free and offers open possibility for chemical end functionalization compared to other reported cell culture proficient modified dipeptide-based hydrogels. In addition, incorporation of an unnatural amino acid ΔF in the gelling motif would provide the hydrogel with enhanced stability to resist enzymatic degradation (26) and hence longer cell culture half-life as compared to simple dipeptide based hydrogels. Finally, the fact that the dipeptide gel described here could be easily derivatized with a specific peptide based ligand opens the door for its derivatization with other ligands for the development of suitable hydrogels promoting long term 3D growth and expansion of cells for tissue engineering as well as cell biological applications.

5. CONCLUSIONS

In this work, we have described 3D growth and proliferation of mammalian cells on an easy to functionalize and biocompatible dipeptide hydrogel. When covalently linked with an RGD containing pentapeptide, the gel supported attachment and growth of mammalian cells for a relatively long time period, in a way better than the underivatised hydrogel. The gel also permitted 3D growth of cells with cell invasion taking place throughout the scaffold which would assist in achieving increased efficiency and specificity of cellular growth by better modeling in vivo growth environments. These results and the inherent properties of FΔF gel such as increased resistance to enzymatic degradation, responsiveness to environmental changes (pH, salt concentration etc.) (26), easier gel formation, and ease of derivatization make it an ideal candidate for the development of a more complex 3D scaffold with effective cellular growth compared to other reported small peptide-based hydrogels to date (22−25).

Acknowledgment. J.J.P. thanks the Indian Council of Medical Research and A.S. thanks the Council for Scientific and Industrial Research for fellowships. Authors thank the core funding at International Centre for Genetic Engineering and Biotechnology, New Delhi, and Department of Biotechnology, India, for financial assistance; Mrs. Rashmi Srivastav, ICGEB, New Delhi, for mass spectroscopic analysis; and Dr. Paushali Mukherjee for her guidance in carrying out the cell culture studies.

Supporting Information Available: HPLC profiles and mass spectroscopy results of the peptides, optical bright-field and live/dead fluorescent images of cells cultured on gels and tabular results showing cell viability and gel penetration (PDF).This material is available free of charge via the Internet at http://pubs.acs.org.

REFERENCES AND NOTES

(1) Cushing, M. C.; Anseth, K. S. *Science* **2007**, *316*, 1133–4.
(2) Alberts, B.; Johnson, A.; Lewis, J.; Raff, M.; Roberts, K.; Walter, P. *Molecular Biology of the Cell*, 4th ed.; Garland Publishing: New York, 2002.
(3) Freeman, W. H. In *Molecular Cell Biology*, 5th ed.; Scott, M., Matsudaira, P., Lodish, H., Darnell, J., Zipursky, L., Kaiser, C., Eds.; W. H. Freeman: San Francisco, CA; 2003.
(4) Behonick, D. J.; Werb, Z. *Mech. Dev.* **2003**, *120*, 1327–36.
(5) Discher, D. E.; Janmey, P.; Wang, Y. L. *Science* **2005**, *310*, 1139–43.
(6) Jen, A. C.; Wake, M. C.; Mikos, A. G. *Biotechnol. Bioeng.* **1996**, *50*, 357–64.
(7) Lysaght, M. J.; Aebischer, P. *Sci. Am.* **1999**, *280*, 76–82.
(8) Lee, K. Y.; Mooney, D. J. *Chem. Rev.* **2001**, *101*, 1869–79.
(9) Bryant, S. J.; Anseth, K. S.; Lee, D. A.; Bader, D. L. *J. Orthop. Res.* **2004**, *22*, 1143–9.
(10) Kisiday, J.; Jin, M.; Kurz, B.; Hung, H.; Semino, C.; Zhang, S.; Grodzinsky, A. J. *Proc. Natl. Acad. Sci. U.S.A.* **2002**, *99*, 9996–10001.
(11) Fisher, J. P.; Jo, S.; Mikos, A. G.; Reddi, A. H. *J. Biomed. Mater. Res., A* **2004**, *71* (12), 268–74.
(12) Liu, V. A.; Bhatia, S. N. *Biomed. Microdev.* **2002**, *4*, 257–266.
(13) Shin, H.; Zygourakis, K.; Farach-Carson, M. C.; Yaszemski, M. J.; Mikos, A. G. *J. Biomed. Mater. Res., A* **2004**, *69*, 535–43.
(14) Alhadlaq, A.; Elisseeff, J. H.; Hong, L.; Williams, C. G.; Caplan, A. I.; Sharma, B.; Kopher, R. A.; Tomkoria, S.; Lennon, D. P.; Lopez, A.; Mao, J. J. *Anals of Biomed. Eng.* **2004**, *32*, 911–923.
(15) Holmes, T. C. *Trends Biotechnol.* **2002**, *20*, 16–21.
(16) Ruoslahti, E. *Annu. Rev. Biochem.* **1988**, *57*, 375–413.
(17) Ruoslahti, E.; Pierschbacher, M. D. *Science* **1987**, *238*, 491–7.
(18) Yamada, K. M. *J. Biol. Chem.* **1991**, *266*, 12809–12.
(19) Bokhari, M. A.; Akay, G.; Zhang, S.; Birch, M. A. *Biomaterials* **2005**, *26*, 5198–208.
(20) Silva, G. A.; Czeisler, C.; Niece, K. L.; Beniash, E.; Harrington, D. A.; Kessler, J. A.; Stupp, S. I. *Science* **2004**, *303*, 1352–5.
(21) van Bommel, K. J. C.; van der pol, C; Muizebelt, I.; Friggeri, A.; Heeres, A.; Meetsma, A.; Feringa, B. L.; van Esch, J. *Angew. Chem., Int. Ed.* **2004**, *43*, 1663–1667.
(22) Jayawarna, V.; Richardson, S. M.; Hirst, A. R.; Hodson, N. W.; Saiani, A.; Gough, J. E.; Ulijn, R. V. *Acta. Biomater.* **2009**, *5*, 934–43.
(23) Jayawarna, V.; Ali, M.; Jowitt, T. A.; Miller, A. F.; Saiani, A.; Gough, J. E.; Ulijn, R. V. *Adv. Mater.* **2006**, *18*, 611–614.
(24) Liebmann, T.; Rydholm, S.; Akpe, V.; Brismar, H. *BMC Biotechnol.* **2007**, *7*, 88.
(25) Jayawarna, V.; Smith, A.; Gough, J. E.; Ulijn, R. V. *Biochem. Soc. Trans.* **2007**, *35*, 535–7.
(26) Panda, J. J.; Mishra, A.; Basu, A.; Chauhan, V. S. *Biomacromolecules* **2008**, *9*, 2244–50.
(27) Ho, M. H.; Wang, D. M.; Hsieh, H. J.; Liu, H. C.; Hsien, T. Y.; Lai, J. Y.; Hou, L. T. *Biomaterials* **2005**, *26*, 3197–206.
(28) Steffens, G. C.; Nothdurft, L.; Buse, G.; Thissen, H.; Hocker, H.; Klee, D. *Biomaterials* **2002**, *23*, 3523–31.
(29) Kouvroukoglou, S.; Dee, K. C.; Bizios, R.; McIntire, L. V.; Zygourakis, K. *Biomaterials* **2000**, *21*, 1725–33.
(30) Grabarek, Z.; Gergely, J. *Anal. Biochem.* **1990**, *185*, 31–5.
(31) Gupta, M.; Bagaria, A.; Mishra, A.; Mathur, P.; Basu, A.; Ramakumar, S.; Chauhan, V. S. *Adv. Mater.* **2007**, *19*, 858.
(32) Francis, S. E.; Goh, K. L.; Hodivala-Dilke, K.; Bader, B. L.; Stark, M.; Davidson, D.; Hynes, R. O. *Arterioscler. Thromb. Vasc. Biol.* **2002**, *22*, 927–33.
(33) Mosmann, T. *J. Immunol. Methods* **1983**, *65*, 55–63.
(34) Ayad, S.; Boot-Handford, R. P.; Humphreise, M. J.; Kadler, K. E.; Shuttleworth, C. A. *The Extracellular Matrix: Facts Book*, 2nd ed.; Academic Press: San Diego, CA, 1998.
(35) Kreis, T.; Vale, R. *Guide Book to the Extracellular Matrix, Anchor, And Adhesion Proteins*, 2nd ed.; Oxford University Press: Oxford, U.K., 1999.
(36) Zhang, S.; Gelain, F.; Zhao, X. *Semin. Cancer Biol.* **2005**, *15*, 413–20.
(37) Healy, K. E.; Tsai, D.; Kim, J. E. *Mater. Res. Soci. Symp. Proc.* **1992**, *252*, 109.
(38) Whang, K.; Thomas, C. K.; Nuber, G.; Healy, K. E. *Polymer* **1995**, *36*, 837.
(39) Massia, S. P.; Hubbell, J. A. *J. Cell Biol.* **1991**, *114*, 1089–100.
(40) Giancotti, F. G. *Nat. Cell. Biol.* **1999**, *2*, E13.
(41) Chen, C. S.; Mrksich, M.; Huang, S.; Whitesides, G. M.; Ingber, D. E. *Science* **1997**, *276*, 1425–8.
(42) Tan, J.; Gemeinhart, R. A.; Ma, M.; Saltzman, W. M. *Biomaterials* **2005**, *26* (17), 3663–71.
(43) Fischbach, C.; Kong, H. J.; Hsiong, S. X.; Evangelista, M. B.; Yuen, W.; Mooney, D. J. *Proc. Natl. Acad. Sci. U.S.A.* **2009**, *106*, 399–404.
(44) Holmes, T. C.; de Lacalle, S.; Su, X.; Liu, G.; Rich, A.; Zhang, S. *Proc. Natl. Acad. Sci. U.S.A.* **2000**, *97*, 6728–33.
(45) Kretsinger, J. K.; Haines, L. A.; Ozbas, B.; Pochan, D. J.; Schneider, J. P. *Biomaterials* **2005**, *26*, 5177–5186.
(46) Ferreira, L. S.; Gerecht, S.; Fuller, J.; Shieh, H. F.; Vunjak-Novakovic, G.; Langer, R. *Biomaterials* **2007**, *28*, 2706–17.
(47) Hahn, M. S.; Miller, J. S.; West, J. L. *Adv. Mater.* **2006**, *18*, 2679–2684.
(48) Langer, R.; Vacanti, J. *Tissue Eng. Sci.* **1993**, *260*, 920.
(49) Underhill, G. H.; Chen, A. A.; Albrecht, D. R.; Bhatia, S. N. *Biomaterials* **2007**, *28*, 256–70.
(50) Shin, Y. M.; Kim, K. S.; Lim, Y. M.; Nho, Y. C.; Shin, H. *Biomacromolecules* **2008**, *9*, 1772–81.
(51) Smith, A. G.; Britland, S. T.; Crowther, N. J.; Eagland, D. *Eur. Cells Mater.* **2002**, *4*, 91–92.

AM1005173